Effect of Effective Velocity Ratio on the Near-Field Mixing Structures of a Jet in Crossflow

Peerati Watakulsin, Woraboot Gimjaiyen, Wasin Saengnumpong, Anusarn Sangnimnuan, Alongkorn Pimpin and Asi Bunyajitradulya*

Department of Mechanical Engineering, Faculty of Engineering, Chulalongkorn University
Bangkok 10330, Thailand

* Corresponding Author: Tel: 02 218 6645, Fax: 02 218 6645, E-mail: asi.b@chula.ac.th

Abstract

The effect of jet-to-crossflow effective velocity ratio (r) on the near-field mixing structures of a jet in crossflow is investigated. Three jets with r of 2, 4, and 7 are examined under the condition of equal jet volume flowrate and equivalent stoichiometric ratio. The experiment is conducted using the combination of smoke fluid condensation, Mie scattering, and laser-sheet visualization techniques. Series of planar laser-sheet visualization images, particularly the plane perpendicular to the jet exit, are taken. The instantaneous and mean images are then analyzed in order to survey the effect of r on the near-field mixing structures. It is found that as r increases, the mean mixing structure of the jet changes characteristics from the lateral-maximum, leewardly-connected, two distinct lateral lobes at the extreme low-r, r = 2, to windward-maximum, windwardly-connected structure at the extreme high-r, r = 7. For the intermediate r, r = 4, it is found that such evolution occurs spatially. That is, the jet at r = 4 evolves from the characteristics of the extreme high-r jet to those of the extreme low-r jet in the transverse direction. These results suggest that the near-field mixing structures of a jet in crossflow, in the region where the unmixed core is still present, can be described by the competing effect between the developments of 1) the lateral skewed mixing layers and the corresponding vortical roll ups and 2) the windward jet shear layer. Specifically, when consider the evolution with respect to increasing r, JICF evolves from the lateral skewed mixing layers dominated in the low-r jet to the windward jet shear layer 'dominated' in the high-r jet. On the other hand, such reverse evolution, i.e., in the direction of decreasing r, occurs spatially for the intermediate-r jet as the jet evolves in the transverse direction.

Keywords: jet in crossflow, effective velocity ratio, mixing, entrainment, near-field structures

1. Introduction

This paper reports our continued efforts [1-4] in the study of jets in crossflow (JICF). Here, we attempt to address the issue of the effect of the jet-to-crossflow effective velocity ratio (r) on mixing and mixing structures of the jet, particularly in the near-field where the jet unmixed core is still present. The jet-to-crossflow effective velocity ratio is defined as the square root of the jet-to-crossflow momentum flux ratio, $r = \sqrt{\rho_j u_j^2 / \rho_{cf} u_{cf}^2}$, where ρ is density, u is velocity, and subscripts j and cf refer to jet and crossflow, respectively.

In this respect, past studies have made considerable progress towards the understanding of a jet in crossflow in general, see, for example, [5-8]. Naturally, fewer addressed the issue of the effect of r on the jet, and even fewer on the effect of r on the jet mixing and mixing structures. Of most relevant at present is the work of Smith and Mungal [5]. Smith and Mungal used acetone-PLIF technique, which marks passive-scalar structures, to study jets in crossflow for r = 5, 10, 15, 20, and 25. They found many important results; among others, 1) the lower-r jet (r = 5) has different characteristics from the higher-r jets and is believed to belong to a different flow regime; 2) the vortex interaction region shows r-dependent variations in the flow field, including specifically a slower development of the counter-rotating vortex pair (CVP) in higher-r jets. While these results are vital and important, due to the technique used it did not mark the mixing regions and structures in the flow directly. With this in mind, the present study attempts to complement the work of Smith and Mungal by investigating the effect of r on mixing and mixing structures in the near-field of a jet in crossflow, under the condition of equal jet volume flowrate and equal equivalent stoichiometric ratio. To give some indication of mixing and mixing structures, a combination of smoke-fluid condensation, MIE scattering, and laser-sheet visualization techniques is employed, see [2,3]. Besides this difference in mixing aspect, the present study addresses the effect of r in the lower range, from 2 to 7, than those of Smith and Mungal.

2. Experiment

The configuration of a jet in crossflow is shown in Fig. 1, together with the coordinate axes employed: x, streamwise; y, traverse; z, spanwise, with the origin at the jet center in the jet exit plane. For convenience, we shall refer to the planes perpendicular to the x, y, and z axes as end, top, and side views, respectively. Figure 1 also indicates seven relevant dimensional variables (ρ, ν, and u of jet and crossflow, where ν is kinematic viscosity; and d, the diameter of the jet) and one generic dependent dimensionless mixing parameter ψ, considered in the present experiment.

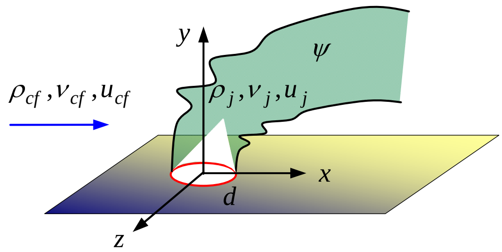

Fig. 1. Configuration of a jet in crossflow and relevant properties considered.

Under this limited scope of variables, and for 1) specified and fixed equivalent jet-to-crossflow stoichiometric ratio St (and/or entrainment ratio), 2) specified and fixed thermodynamic states of jet and crossflow, and 3) fixed jet condition (volume flowrate, diameter, initial velocity profile, etc.), from dimensional argument we have $\psi = f(r;St)$. Note that we may define St as, for example, the entrained and mixed crossflow-fluid to jet-fluid flowrate ratio. Note also that under these conditions, r and the crossflow Reynolds number Re_{cf}, defined by $\mathrm{Re}_{cf} = u_{cf} d / \nu_{cf}$, have a one-to-one correspondence. As a result, the present result can equally be interpreted as the effect of the crossflow Reynolds number, $\psi = f(\mathrm{Re}_{cf}; St)$.

It should be mentioned that the above dimensional argument is a simplified one. Past studies have shown that there are other parameters that can affect the characteristics of a jet in crossflow to various degrees; examples are jet initial velocity profile and crossflow boundary layer condition, see, e.g., [8]. In the present study, we keep these other conditions fixed.

2.1. Experimental Setup and Technique

The flow facility is the same open-circuit blower tunnel and JICF setup as that described in [1]. Briefly, the jet, whose inner diameter at exit measured 32 mm, is flushed-mounted to the test section floor. The jet exit velocity profile is top-hat with slight dip at the center. For further details, see [1].

In order to visualize the mixing and the mixing structures – especially in the near field, the combination of smoke fluid condensation, Mie scattering, and laser-sheet visualization techniques, as described in [2,3] and illustrated in Fig. 2, is used. Specifically, a heated jet seeded with *vaporized* smoke fluid is used. Briefly, the jet supply air is heated with a heater upstream then seeded with smoke fluid by injection at the location downstream of the heater. The temperature of the jet is adjusted such that it ensures complete evaporation of the smoke fluid before the jet leaves the exit. (See further remark regarding the jet temperature below.) As the jet leaves the exit, and entrains and mixes with the cooler crossflow fluid to the predetermined equivalent stoichiometric ratio St,

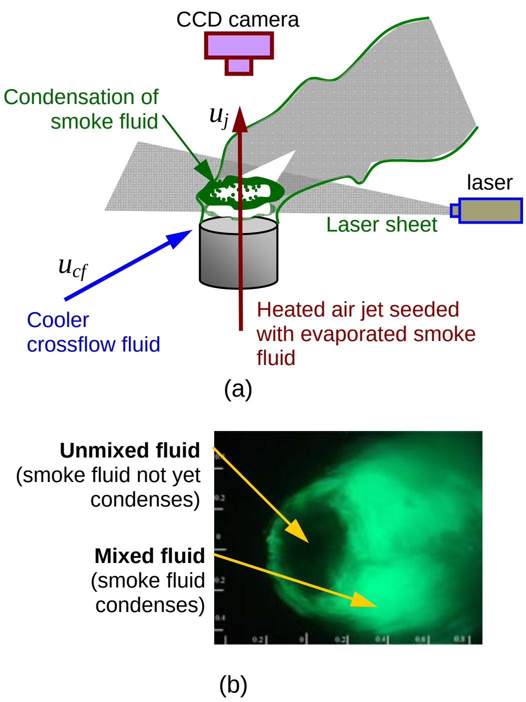

Fig. 2. (a) A diagram illustrating the setup of the combination of smoke fluid condensation, MIE scattering, and laser-sheet visualization techniques to visualize mixing.
(b) An example of visualized image showing the surrounding mixed region and the unmixed core region in the plane perpendicular to the jet exit.

the smoke fluid condenses into aerosol particles. With planar laser-sheet visualization, the aerosol particles act as scattering tracers that mark the region and structure of mixing in the near field. On the contrary, in the region where the jet is not yet fully mixed with the crossflow to the stoichiometric ratio, especially in the jet core region, there are no condensed aerosol particles and thus no scattering signal, signifying the region of not yet fully mixed fluid.

A few points regarding the current technique should be noted. Firstly, because the near-field mixing structures – preferably very close to the jet exit plane – are desired, care must be taken in adjusting the jet exit temperature. Specifically, 1) on the one hand, the jet temperature must be high enough such that the smoke fluid is completely evaporated in the supply pipe before the jet exits at the exit plane, 2) on the other hand, it must not be too high such that condensation occurs too far away from the exit plane and the near-field mixing structures near the jet exit plane cannot be captured. Secondly, here the 'equivalent stoichiometric ratio' is achieved through equal jet volume flowrate and equal jet exit temperature. As mentioned above, since the near-field mixing structures very close to the jet exit plane are desired, our 'predetermined' stochiometric ratio is therefore fixed by the entrainment and mixing capability of the current jet. If so desired, visualization of the mixing structures at a larger crossflow-to-jet stoichiometric ratio is possible via the raising of the jet exit temperature, naturally at the expense of not being able to capture the structure very near the jet exit. Thirdly, it is necessary to note that while the current technique is expected to give reasonable indication of intense mixing region in the near field, it is not expected to be so further away where the jet fluid is already fully mixed with the crossflow fluid to the stoichiometric ratio, the smoke fluid is already condensed, and there is no more 'production' of the aerosols. Under the current technique, the process in these far regions is more appropriately considered as entrainment and dilution, rather than entrainment and mixing. (In this regard, the near-field region is also contaminated by dilution to an extent.) Therefore, the current focus is in the region from the plane very close to the jet exit to the plane at the end of the unmixed jet core, where the jet is considered fully mixed with the crossflow to the stoichiometric ratio.

2.2. Experimental Condition

The experiment is conducted for the effective velocity ratios of 2, 4, and 7. Throughout the experiment, the velocity, temperature, and condition of the jet are kept fixed, while the crossflow velocity is varied in order to achieve different effective velocity ratio. The corresponding crossflow Reynolds number Re_{cf} are 14,000, 7,000, and 4,000, respectively, while the jet Reynolds number $\mathrm{Re}_j = u_j d / \nu_j$ is 21,000. The jet center temperature, measured at the jet exit plane when the smoke fluid is turned on and the crossflow is turned off, is 130 ^{o}C; the crossflow temperature is 31 ^{o}C. The smoke fluid to jet mass flowrate ratio is approximately 0.025. Note that since the initial velocity profile is top-hat, the area average velocity is used in the determination of the jet Reynolds number.

Series of 3-minute video clips of the jet are taken, resulting in a total of 3,000 images for each clip. The statistics are based on this sample of images.

3. Results and Discussion

To give an overview of the jets, the instantaneous and mean images of the side view of the jet in the center plane (z/rd = 0) for all r's are shown in Fig. 3. As expected, the jet with higher r is more upright and penetrates deeper into the crossflow when measured in the physical-, or d-scale. Note that, for a jet with higher r, the same transverse location measured in the rd-scale corresponds to the further transverse location measured in the d-scale. Among others, the jet unmixed core near

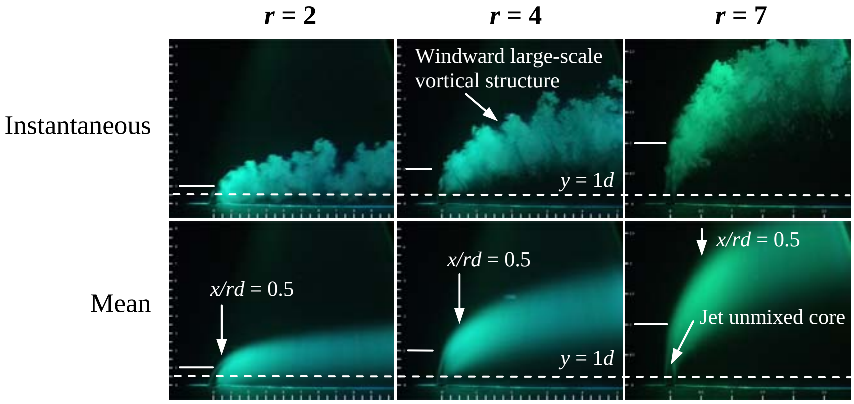

Fig. 3. Side view. Instantaneous and mean images in the center plane (z/rd = 0). For reference, a long dashed line across all three images indicates the location $y = 1d$ for d -scale, while a short solid horizontal line in front of each jet indicates the location $y = 1rd$ for the rd -scale.

the jet exit and the large-scale structures on the windward side are clearly observed. Note that there is a slight variation in the laser condition which results in slightly different laser sheet color. Note also that in this center-plane side view, any lateral activity cannot be captured.

3.1. Instantaneous Mixing Structures

Figure 4 shows the instantaneous images in the top view from y/rd = 0.05 to 0.6: 4a, the evolution of the mixing structures in rd -scale; 4b, the comparison of the mixing structures in d -scale. For the extreme low- r jet, r = 2, besides the *mixing ring* surrounding the jet unmixed core as reported in [2,3], some mixing structures in the wake region downstream of the jet are clearly observed as early as at y/rd = 0.05. This is not the case for the higher- r jets, r = 4 and 7. As we move further up at y/rd = 0.1, a pair of lateral-leeward vortical roll ups (LLVR) - one on each lateral side relative to the jet unmixed core - starts to appear. They can be seen more clearly and are already well developed at y/rd = 0.15, where the jet unmixed core is still present. The cusps at the lateral sides, pointed by arrows at y/rd = 0.1 and 0.15, appear to be the point of inception of the LLVR. However, the development of the skewed mixing layer around the jet exit column is expected to start azimuthally upstream of this point. As we move further up, this pair of mixing structures clearly dominates and is identified as part of the counter-rotating vortex pair (CVP) from the end view image (not shown). In this regard, we note that we observe the CVP from the end view image right at our first imaging location downstream of the jet center, at x/rd = 0.5 (see Fig. 3); no end-view data are available upstream of this location.

For r = 4, similar structures and results as reported in [2,3] are observed. To recap, the instantaneous images show three dominant instantaneous mixing structures: (1) the cascading azimuthal Kelvin-Helmholtz (K-H) mixing structures around the jet column, (2) the leeward vortical roll ups (LVR), and (3) the windward vortical roll ups (WVR). The cascading K-H structures are initiated and develop early on near the leading edge on the windward side of

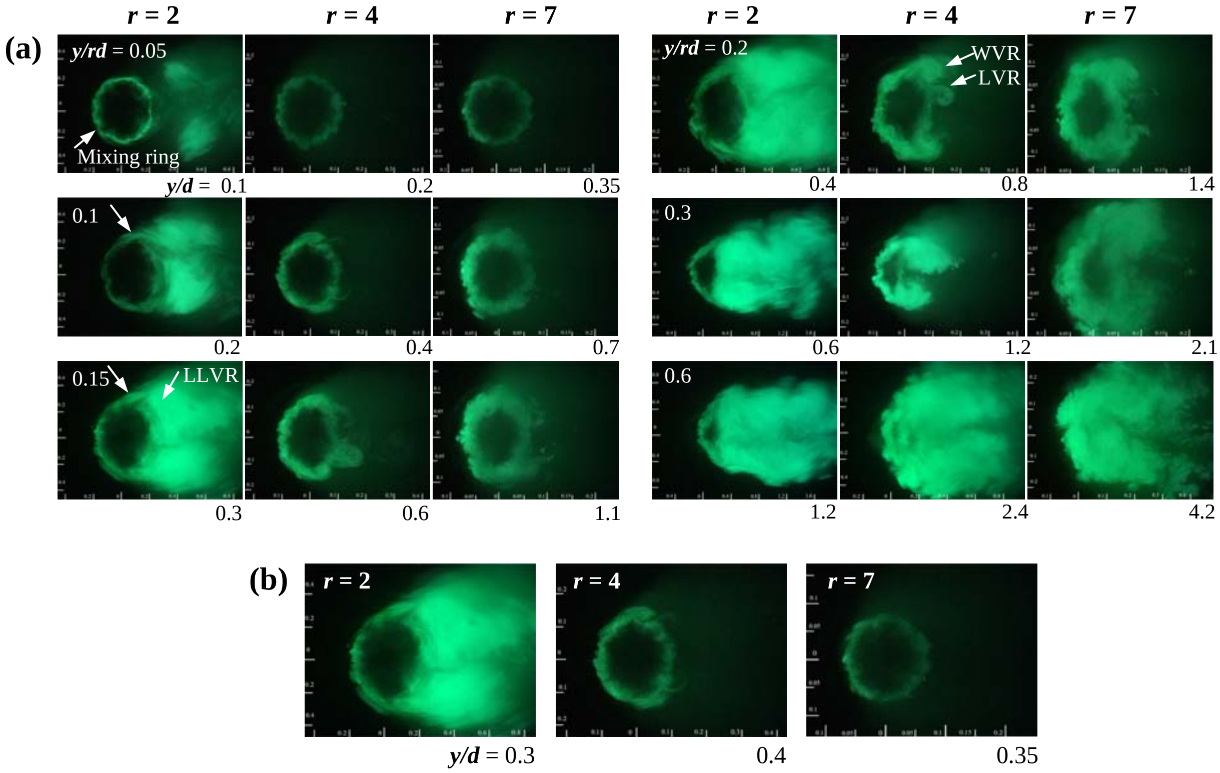

Fig. 4. Top view. Instantaneous mixing structures. The streamwise direction is from left to right. The fields of view may not be the same. Zoom in to see the rd -scale on each image.

(a) Evolution of the mixing structures in rd -scale.

(b) Comparison of the mixing structures in d -scale.

the jet column. These structures are responsible for the mixing in the very near field region. Further away, the windward vortical roll ups – as opposed to the leeward ones – predominantly govern entrainment and mixing and develop into the CVP. Similar development of the lateral vortical roll ups is observed for r = 7 although it is now more difficult to identify whether there are the corresponding windward and leeward vortical structures. For simplicity, here we shall refer to the dominant lateral vortical roll ups in all cases simply as the lateral vortical roll ups.

When we compare the developments of these lateral vortical roll ups in rd -scale in Fig. 4a, we see that the lateral vortical roll ups in the extreme low-r jet, r = 2, are already well-developed at y/rd = 0.15, while those for the higher-r jets develop much later. If we are to compare these developments in d -scale, this translates into an even faster development for the extreme low-r jet. The comparison in d -scale, at $y/d \approx 0.3$, is highlighted in Fig 4b. These results show that the lateral vortical roll ups and the corresponding CVP in the lower-r jet form and develop faster than those in the higher-r jet. This is in agreement with the result of Smith and Mungal [5]. It should be pointed out that Smith and Mungal used acetone-PLIF technique, which observes passive scalar structures, while the present study uses condensation, which observes more directly mixing structures, and that Smith and Mungal studied JICF for r = 5, 10, 15, 20, and 25, a higher r range than the current study. The present result therefore complements the past result of Smith and Mungal.

3.2. Mean Mixing Structures

In order to study the mixing structures in further detail, the mean results are shown in Fig. 5. Figure 5a shows the normalized mean contour and representative mean images. The mean is normalized by the maximum value in the plane, thus the value ranges from low values to one.

Firstly, the faster development of the lateral vortical roll ups for the lower-r jet discussed in the last section is observed and confirmed in the mean structures. Specifically, for the extreme low-r jet the two lateral vortical roll ups are already well developed at y/rd =

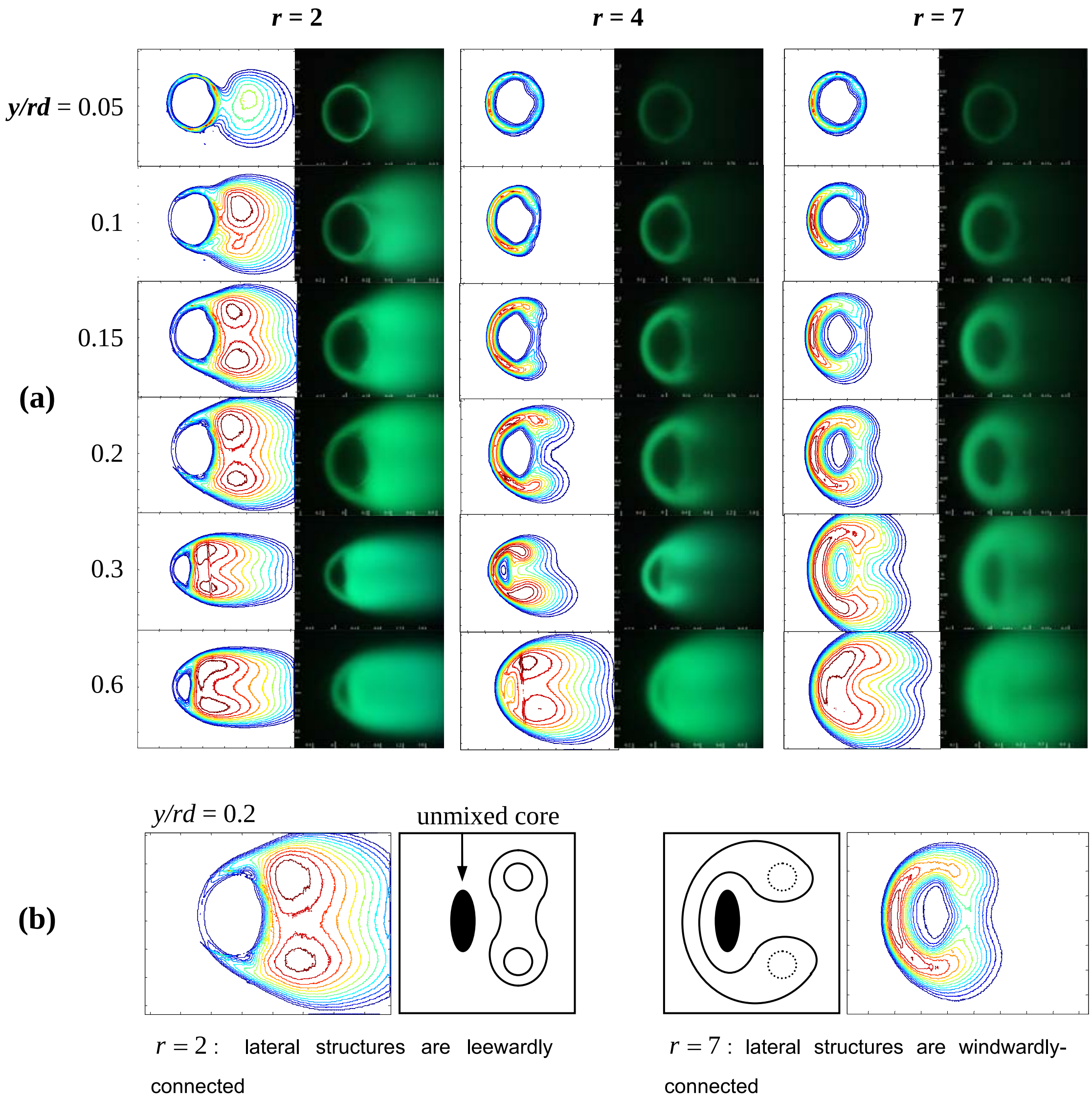

Fig. 5. (a) Top View. Normalized mean contours and representative mean images.
[Red contours are high values close to 1, blue contours are low values 0.4 up. The corresponding sizes and positions of the images are *not* scaled relative to each others.]
(b) Two types of connectedness of the lateral vortical roll ups: leewardly-connected in the extreme low-r jet and windwardly-connected in the extreme high-r jet.

0.15, where the unmixed core is still present, while those of higher-r jets are not yet developed until much further transverse location. Additional effects of r on the mean mixing structures can be observed as follows.

Firstly, at y/rd = 0.15, for the extreme low-r jet, r = 2, the maximum value of the mean is on each lateral (relative to the jet unmixed core) side, the location of the lateral vortical roll ups. This indicates that there are strong mixing activities in these roll ups. This is further supported by the large and maximum value of the fluctuation, indicated by the normalized standard deviation (not shown here), in these roll ups. In contrast, for the extreme high-r jet, r = 7, the maximum value occurs on the windward side, the location of the windward jet shear layer. Similar trend of high and maximum value on the windward side for this extreme high-r jet is also observed in the normalized standard deviation.

Secondly, for the extreme low-r jet, starting around y/rd = 0.15, the two lateral vortical roll ups result in two clearly distinct (mean) lateral lobes – predominantly connected via the structure *leeward of the jet unmixed core*. (This can be contributed to vortex interaction.) On the other hand, for the extreme high-r jet, while two lateral vortical roll ups might result in two weakly distinct (with local peaks) lateral lobes at further up location, unlike those of the extreme low-r jet, however, the lateral vortical roll ups and the corresponding lobes appear to be predominantly connected via the structures *windward of the jet unmixed core*. (The location of the windward jet shear layer.) This difference in the structure connectedness between the extreme low-r jet and the extreme high-r jet is highlighted in Fig. 5b. Finally, the lateral-maximum, leewardly-connected, two distinct lateral lobes trend for the extreme low-r jet continues from y/rd = 0.15 further up in the transverse direction, while the windward-maximum, windwardly-connected trend for the extreme high-r jet similarly continues further up.

As for the intermediate r jet, r = 4, the result shows that the mean structure in this case evolves from windward-maximum, windwardly-connected structure of the extreme high-r jet to the lateral-maximum, leewardly-connected, two distinct lateral lobes of the extreme low-r jet as the jet evolves in the transverse direction. This can be clearly seen from its evolution from y/rd = 0.15 to 0.6, the region where the unmixed core is still present.

4. Conclusions

The effect of jet-to-crossflow effective velocity ratio (r) on the near-field mixing structures of a jet in crossflow is investigated for r = 2, 4, and 7. The investigation is carried out only in the near-field where the jet unmixed core is still present. It is found that as r increases, the mean mixing structure of the jet changes characteristics from the lateral-maximum, leewardly-connected, two distinct lateral lobes at the extreme low-r, r = 2, to windward-maximum, windwardly-connected structure at the extreme high-r, r = 7. For the intermediate r, r = 4, it is found that such evolution occurs spatially. That is, the jet at r = 4 evolves from the characteristics of the extreme high-r jet to those of the extreme low-r jet in the transverse direction.

These results suggest that the near-field mixing structures of a jet in crossflow, in the region where the unmixed core is still present, can be described by the competing effect between the developments of 1) the lateral skewed mixing layers and the corresponding vortical roll ups and 2) the windward jet shear layer. Specifically, when consider the evolution with respect to increasing r, JICF evolves from the lateral skewed mixing layers dominated in the low-r jet to the windward jet shear layer 'dominated' (to an extent described below) in the high-r jet. On the other hand, such reverse evolution (decreasing r) occurs spatially in the transverse direction for the intermediate-r jet.

The above results are consistent with the larger strength of the skewed mixing layers in the lower-r jet when comparing the jets with different r, and the spatially increasing strength of the skewed mixing layers in a jet as the jet evolves spatially and gradually loses its transverse momentum in any one jet.

While for the extreme low-r jet ($r=2$), it is seen from the mean structures in Fig. 5 that the skewed mixing layers and the subsequent lateral vortical roll ups dominate the mixing, the role of the windward jet shear layer at the extreme high-r ($r=7$) summarized above as 'dominated' needs further elaboration. Specifically, as r increases, the role of the windward jet shear layer in mixing clearly increases as shown by 1) the shifting of the location of the maximum mean value and standard deviation from the lateral side to the windward side, 2) the shifting of the connectedness of the structures from leewardly-connected to windwardly-connected, and 3) the relative increase in windward contribution to the mean mixing structures, whether the windward jet shear layer contributes more to the overall mixing in the extreme high-r jet ($r=7$) is still not yet as clear from the present data. Thus, by windward jet shear layer 'dominated' here we refer mainly to the three attributes above.

Finally, we obtain the results along the same line, but with respect to the mixing structures and lower range of r, as those of Smith and Mungal [5]. Specifically, we found that the lower-r jet has different characteristics from the higher-r jet and that the lower-r jet has faster development of the lateral vortical roll ups and the corresponding counter-rotating vortex pair (CVP).

5. Acknowledgement

The current research is funded by The Thailand Research Fund and The Commission on Higher Education under the Grant No. RMU5080047. The funding is gratefully acknowledged.

6. References

1. Bunyajitradulya, A. and Sathapornnanon, S. (2005), Sensitivity to Tab Disturbance of the Mean Flow Structure of Nonswirling Jet and Swirling Jet in Crossflow, *Phys. Fluids* 17, 045102.
2. Chongsiripinyo, K., Limdumrongtum, P., Pimpin, A., and Bunyajitradulya, A. (2008), Investigation of Mixing Structure in The Near Field of A Jet in Crossflow, *Proceedings of The Twenty-Second Conference of Mechanical Engineering Network of Thailand*, 15-17 October 2008, Thammasat University, Rangsit Campus, Pathum Thani, Thailand.

3. Limdumrongtum, P., Chongsiripinyo, K., Nontiwatwanich, P., Pimpin A., Bunyajitradulya, A. (2009), Investigation of Mixing Structure in The Near Field of Swirling Jets in Crossflow, *Proceedings of The Twenty-Third Conference of Mechanical Engineering Network of Thailand*, November 4 – 7, 2009, Chiang Mai, Thailand.
4. Kornsri, P., Pimpin, A., and Bunyajitradulya, A. (2009), A Scheme for The Manipulation and Control of A Jet in Crossflow: The Use of Azimuthal Control Jets, *Proceedings of The Twenty-Third Conference of Mechanical Engineering Network of Thailand*, November 4 – 7, 2009, Chiang Mai, Thailand.
5. Smith, S. H. and Mungal, M. G. (1998), Mixing, Structure and Scaling of the Jet in Crossflow, *J. Fluid Mech.*, Vol. 357, pp. 83-122.
6. Yuan, L. L., Street, R. L., and Ferziger, J. H. (1999), Large-Eddy Simulations of A Round Jet in Crossflow, *J. Fluid Mech.*, Vol. 379, pp. 71-104.
7. Kelso, R. M., Lim, T. T., and Perry, A. E. (1998), New Experimental Observations of Vortical Motions in Transverse Jets, *Phys. Fluids*, Vol. 10, No. 9, pp. 2427-2429.
8. Muppidi, S. and Mahesh, K. (2005), Study of Trajectories of Jets in Crossflow Using Direct Numerical Simulations, *J. Fluid Mech.*, Vol. 530, pp. 81-100.